Electronic Factors for Protonation of an Organometallic Molecule. Photoelectron Spectroscopy and Electron Paramagnetic Resonance Study of $[(\eta^6\text{-}C_6H_6)Mo(TRIPOD)]^{0/+}$

Victor S. Asirvatham,[1] Nadine E. Gruhn,[2] Dennis L. Lichtenberger,[2] and Michael T. Ashby*,[1]

Department of Chemistry and Biochemistry, The University of Oklahoma, 620 Parrington Oval, Room 208, Norman, Oklahoma 73019-0370, and Center for Gas-Phase Electron Spectroscopy, Department of Chemistry, University of Arizona, Tucson, Arizona 85721-0041

Received August 23, 1999

We have previously shown that the arene complex $(\eta^6\text{-}C_6H_6)Mo(TRIPOD)$, where TRIPOD = 1,1,1-tris((diphenylphosphino)methyl)ethane, is protonated by *exo* addition of H^+ to the arene ring to give the transient cyclohexadienyl complex $[(\eta^5\text{-}C_6H_7)Mo(TRIPOD)]^+$, which eventually yields the thermodynamic molybdenum hydride $[(\eta^6\text{-}C_6H_6)Mo(TRIPOD)(H)]^+$. The present study is a combined experimental and theoretical investigation that reveals the fundamental basis for this mechanism. Photoelectron spectroscopy (PES) is used to probe the electronic structure of $(\eta^6\text{-}C_6H_6)Mo(TRIPOD)$ and the production of the $[(\eta^6\text{-}C_6H_6)Mo(TRIPOD)]^+$ cation in the gas phase. The initial ionizations of $(\eta^6\text{-}C_6H_6)Mo(TRIPOD)$ are from energetically closely spaced orbitals of predominantly metal d character ($^2A_1$ and ^2E cation states using C_{3v} symmetry) that are shifted over 2 eV to lower energy with respect to the comparable ionizations of $(\eta^6\text{-}C_6H_6)Mo(CO)_3$. The oxidized species $[(\eta^6\text{-}C_6H_6)Mo(TRIPOD)]^+$ is also prepared in solution by electrochemical means and through the use of chemical oxidants. The electron paramagnetic resonance (EPR) spectrum of this cation shows arene-proton hyperfine coupling that indicates substantial arene character in the highest occupied orbital. The photoelectron and EPR spectra both provide evidence for Jahn−Teller distortion of the ^2E positive ion states. Electronic structure calculations show that this distortion involves opening of one L−Mo−L angle, which effectively creates an open coordination site on the metal for the hydride to occupy in the final thermodynamic product. These experimental and computational results show that, in terms of their energy, the e symmetry and a_1 symmetry metal-based orbitals are similarly favored for oxidative protonation directly at the metal. The e symmetry orbital has a portion of its density on the arene ring, making access to this orbital by proton approach to the *exo* position of the arene ring possible. For $(\eta^6\text{-}C_6H_6)Mo(TRIPOD)$, *exo* attack at the arene is favored because the TRIPOD ligand shields the e symmetry orbital from direct attack at the metal by the solvated proton. Thus, *exo* attack is not initiated by proton interaction with an arene-based orbital but is initiated by proton interaction with the arene portion of the same e symmetry orbital that directs attack at the metal. Calculations predict low barriers for both direct attack at the metal and *exo* attack at the arene, with attack at the arene favored for longer metal−proton distances.

Introduction

We have previously reported deuterium tracer studies and kinetic measurements that provided evidence for a mechanism for protonation of $(\eta^6\text{-}C_6H_6)Mo(TRIPOD)$ (**1**) to give the metal−hydride complex $[(\eta^6\text{-}C_6H_6)Mo(TRIPOD)(H)]^+$ (**1·(H$^+$)**), which involves *exo* protonation of the arene ligand to give the cyclohexadienyl transient $[(\eta^5\text{-}C_6H_7)Mo(TRIPOD)]^+$ (**1·(H$^+$)‡**) followed by *endo* proton transfer to the metal (text figure, right):[3]

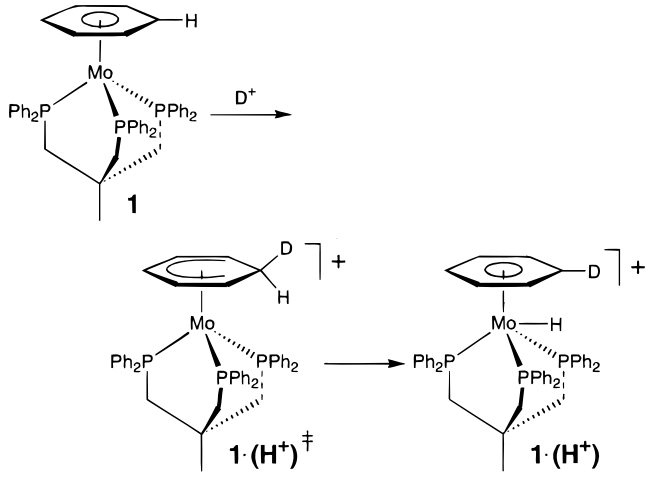

The question naturally arises, why does the proton initially attack the arene ligand to give $[(\eta^5\text{-}C_6H_7)Mo(TRIPOD)]^+$ rather than attack the metal directly to give $[(\eta^6\text{-}C_6H_6)Mo(TRIPOD)(H)]^+$? Protonation of the mol-

(1) The University of Oklahoma.
(2) University of Arizona.
(3) Kowalski, A. S.; Ashby, M. T. *J. Am. Chem. Soc.* **1995**, *117*, 12639.

10.1021/om990673u CCC: $19.00
Publication on Web 05/04/2000

ecule, either at the arene ligand or at the metal center, formally represents an oxidation of the molecule. Initially, the arene ligand, the TRIPOD ligand, and the metal center are all formally neutral in the molecule. Oxidation is expected to occur at the metal center because of the low oxidation potential of molybdenum compared to benzene and phosphines. The formal oxidation state of molybdenum in the final metal−hydride product cation is +II, corresponding to the metal giving up two electrons to the proton to form the hydride. In the cyclohexadienyl transient $[(\eta^5\text{-}C_6H_7)Mo(TRIPOD)]^+$ created by *exo* protonation of the arene ligand, the $\eta^5\text{-}C_6H_7$ ligand has a formal charge of −1, like the familiar $\eta^5\text{-}C_5H_5^-$ ligand, and the metal has again formally given up two electrons to go to the +II oxidation state. Clearly, an understanding of the factors that control protonation of this organometallic molecule requires a more detailed understanding of the electronic structure of the molecule and the characteristics of oxidation and bond formation along the paths of reaction.

The relationship between the protonation of a molecule and the oxidation of that molecule with bonding of a hydrogen atom is explicit in thermodynamics. The protonation energy is equivalent to the ionization energy (IE) of the molecule minus the ionization energy of the hydrogen atom and the homolytic bond energy (BE) to the hydrogen atom as represented by the stepwise process (where negative signs indicate stabilization)

$$M + H^+ \xrightarrow[-\Delta H_{IE}(H)]{\Delta H_{IE}(M)} [M^\bullet]^+ + H^\bullet \xrightarrow{-\Delta H_{BE}([M-H]^+)} [M-H]^+$$

The present paper focuses first on the electronic structure of $(\eta^6\text{-}C_6H_6)Mo(TRIPOD)$ and the energy and bonding capabilities of its one-electron-oxidized derivative $[(\eta^6\text{-}C_6H_6)Mo(TRIPOD)]^+$. The He I and He II photoelectron spectra (PES) of $(\eta^6\text{-}C_6H_6)Mo(TRIPOD)$ provide direct information regarding the relative energies and characters of the positive ion electronic states produced in the gas phase by ionization of the neutral molecule. The one-electron-oxidized derivative $[(\eta^6\text{-}C_6H_6)Mo(TRIPOD)]^+$ has also been prepared chemically and electrochemically, and its electron paramagnetic resonance (EPR) spectra indicate the distribution of the unpaired electron spin in the cation. Electronic structure calculations on both the neutral molecule and the low-lying positive ion states augment the results of the gas-phase photoelectron and solid-state EPR experiments, and calculations along the possible paths of protonation and bond formation show the relation of the experimental results to the energies of reactants, intermediates, transition states, and products. The combination of experiments and calculations offers a simple picture of the features of the electronic structure of $(\eta^6\text{-}C_6H_6)Mo(TRIPOD)$ that control its reactivity toward the proton.

Experimental and Computational Details

Chemicals. The compounds of this study were prepared and handled under an atmosphere of dry nitrogen or argon. $(\eta^6\text{-}C_6H_6)_2Mo$,[4] $(\eta^6\text{-}C_6H_6)Mo(CO)_3$,[5] and $(\eta^6\text{-}1,3,5\text{-}C_6H_3Me_3)Mo(CO)_3$[6] were prepared by published methods. Tetrahydrofuran was predried over P_2O_5, stored over KOH, and then distilled from sodium benzophenone ketal. Dichloromethane was distilled from CaH_2. The other reagents were used as received from Aldrich.

Spectrometers and Other Instruments. ^1H NMR spectra were recorded on a Varian XL-500 instrument using the residual $CHDCl_2$ (5.32 ppm) as an internal standard. ^{31}P NMR spectra were referenced to external 85% H_3PO_4. X-Band EPR spectra were measured using a Bruker EMX spectrometer equipped with an ER 041 XG bridge, an ER 4102ST cavity, and an Oxford liquid He cryostat. Q-band EPR spectra were measured using a Bruker ESP 300E spectrometer equipped with an ER 051Q bridge, an ER 5106QT cavity, and an Oxford liquid He cryostat. The EPR field calibration was checked by measuring the resonance of diphenylpictylhydrazyl radical (dpph). The NMR and EPR samples were prepared in tubes that had been glass-blown onto Schlenk adapters. The solutions were freeze−pump−thawed before the tubes were flame-sealed under vacuum. The PES were recorded using an instrument that has been described previously.[7] The argon $^2P_{3/2}$ ionization at 15.759 eV was used as an internal calibration lock, and the difference between the argon $^2P_{3/2}$ ionization and the methyl iodide $^2E_{1/2}$ ionization at 9.538 eV was used to calibrate the ionization energy scale. During data collection the instrument resolution, measured by using the full width at half-maximum of the argon $^2P_{3/2}$ ionization, was 0.020−0.025 eV.

Synthesis of $(\eta^6\text{-}C_6H_6)Mo(TRIPOD)$. $(\eta^6\text{-}C_6H_6)_2Mo$ (340 mg, 1.35 mmol) and TRIPOD (760 mg, 1.22 mmol) were sealed in a glass tube under vacuum, and the tube was heated at 160 °C for 2 days. The tube was opened under nitrogen, the contents were extracted with 1:1 benzene/heptane (ca. 30 mL), and the extract was filtered. The red-orange product crystallized from the solvent upon cooling to 5 °C for a period of 1 week (620 mg, 64%). ^1H NMR (C_6D_6, 500 MHz, 293 K): δ 1.16 (m, 3 H, CH_3), 2.17 (m, 6 H, CH_2), 4.41 (m, 6 H, C_6H_6), 6.85 (t, J = 7 Hz, 12 H, Ph), 6.96 (t, J = 7 Hz, 6 H, Ph), 7.08 (m, 12 H, Ph). $^{31}P\{^1H\}$ NMR (C_6D_6, 202 MHz, 293 K): δ 46.59 (s). Anal. Calcd (found) for $C_{47}H_{45}P_3Mo$ (798.74): C, 70.68 (70.44); H, 5.68 (5.74).

Synthesis of $[(\eta^6\text{-}C_6H_6)Mo(TRIPOD)]^+$. $(\eta^6\text{-}C_6H_6)Mo(TRIPOD)$ (192 mg, 0.24 mmol) was dissolved in 10 mL of THF, and $AgPF_6$ (61 mg, 0.24 mmol) was added. The solution turns immediately from red to yellow with formation of a gray precipitate. After it was stirred for 10 min, the solution was filtered and then concentrated to ca. 2 mL. Pentane was slowly vapor-diffused into the solution to yield $[(\eta^6\text{-}C_6H_6)Mo(TRIPOD)](PF_6)$ (210 mg, 92%) as yellow-brown crystals. Repeated attempts to characterize $[(\eta^6\text{-}C_6H_6)Mo(TRIPOD)](PF_6)$ by combustion analysis failed to give reproducible results. Freshly prepared crystals of $[(\eta^6\text{-}C_6H_6)Mo(TRIPOD)](PF_6)$ begin turning red-brown after a few hours, even in a glovebox. This may be the result of disproportionation. Single-crystal X-ray diffraction data yielded a reasonable structure for the cation, but the anion was highly disordered (monoclinic, space group $C2$, with a = 18.323(4) Å, b = 24.491(5) Å, c = 10.434 Å, β = 91.28(3)°, Z = 4 at 188 K). Spectral titration with $AgBF_4$ and $FcBF_4$ demonstrated that 1 equiv of the oxidizing agent reacts with $(\eta^6\text{-}C_6H_6)Mo(TRIPOD)$. Attempts to determine the magnetic moment of $[(\eta^6\text{-}C_6H_6)Mo(TRIPOD)](PF_6)$ by the Evans method[8] gave unreasonably high values. EPR (THF, X-band, 4 K): g_x = 2.050), g_y = 2.038, g_z = 1.990; ^{31}P hfc, $a_{xx} = a_{yy}$ = 25 G, a_{zz} = 29 G; ^1H hfc, $a_{xx} = a_{yy} = a_{xx}$ = 5 G; $^{95}Mo/^{97}Mo$ hfc, $a_{xx} = a_{yy} = a_{xx} \approx$ 1 G (unresolved).

Photoelectron Spectra. $(\eta^6\text{-}C_6H_6)Mo(TRIPOD)$ sublimed cleanly at 270−285 °C at 10^{-4} Torr with no detectable evidence of decomposition products in the gas phase or as a solid

(4) Silverthorn, W. E. *Inorg. Synth.* **1977**, *17*, 54.
(5) Nicholls, B.; Whiting, M. C. *J. Chem. Soc.* **1959**, 551.
(6) Angelici, R. J. *Synthesis and Techniques in Inorganic Synthesis*, 2nd ed.; W. B. Sanders: Philadelphia, PA, 1977.
(7) Westcott, B. L.; Gruhn, N. E.; Enemark, J. H. *J. Am. Chem. Soc.* **1998**, *120*, 3382.
(8) Grant, D. H. *J. Chem. Educ.* **1995**, *72*, 39.

residue. The spectra of the free ligand TRIPOD were recorded at 210−230 °C. (η^6-C_6H_6)$Mo(CO)_3$ sublimed at 60−70 °C with evidence of some thermal decomposition. Benzene and CO were observed in the gas phase as contaminants in the spectra, and a black solid residue remained after sublimation was complete. No metal-containing species other than (η^6-C_6H_6)-$Mo(CO)_3$ were observed in the gas phase, and the predominantly metal ionizations of this molecule were not obscured by other species. Ionizations arising from benzene and CO were spectrally subtracted to give the He I spectrum of (η^6-C_6H_6)-$Mo(CO)_3$. (η^6-1,3,5-$C_6H_3Me_3$)$Mo(CO)_3$ sublimed at 95−105 °C without thermal decomposition.

For figures of the photoelectron spectra, the vertical length of each data mark represents the experimental variance of that point. The valence ionization bands are represented analytically with asymmetric Gaussian peaks.[9,10] Bands are defined by the position, amplitude, half-width for the high binding energy side of the peak, and the half-width for the low binding energy side of the peak. The peak positions and half-widths are reproducible to about ±0.02 eV, while the confidence limits for the relative bands areas are about 5%. The number of peaks used in a fit is based solely on the features of a given band profile. The parameters describing an individual ionization peak are less certain when two or more peaks are close in energy and overlap.

Electrochemical Measurements. The cyclic voltammogram (CV) was recorded using a BAS CV50W electrochemical analyzer with a $Ag/AgNO_3$ reference electrode in a cell that has been described earlier.[11] The oxygen-free CH_2Cl_2 solutions employed during the CV measurements were 10^{-3} M in (η^6-C_6H_6)Mo(TRIPOD) and 0.1 M in the supporting electrolyte (n-Bu_4)PF_6. The formal potentials, $E_{1/2}$ values, were determined as the average of cathodic and anodic peak potentials (i.e., $(E_{p,c} + E_{p,a})/2$), and they are referenced versus the ferrocene/ferrocenium couple in CH_2Cl_2 that occurs at 0.46 V versus SCE.[12]

Electron Paramagnetic Resonance. THF solutions of [(η^6-C_6H_6)Mo(TRIPOD)]$^+$ were flash-frozen with liquid N_2 and evacuated before flame-sealing. The entire field was swept during a time period that was approximately 10 times the time constant. The Zeeman modulation amplitude was set to approximately $\sqrt{3}$ times the peak-to-peak line width. The effect of varying the microwave power and the influence of spectrometer amplifier gain were investigated. No additional spectral features were observed using different parameters.

EPR spectral simulations were carried out using the program SimFonia,[13] which uses the following spin Hamiltonian for simulating "powder" EPR spectra:

$$H = \mu_B \cdot B_0 \cdot g_e \cdot \mathbf{S} + \mathbf{S} \cdot \mathbf{D} \cdot \mathbf{S} + \mathbf{S} \cdot \mathbf{A} \cdot \mathbf{I} + \mathbf{I} \cdot \mathbf{P} \cdot \mathbf{I} + \mu_N \cdot B_0 \cdot g_n \cdot \mathbf{I} \quad (1)$$

where μ_B is the Bohr magneton, B_0 is the applied magnetic field, g is the unitless g factor, **S** is the effective spin angular momentum operator, **D** is the matrix of the zero-field splitting tensor, **A** is the nuclear hyperfine interaction tensor, **I** is the nuclear spin vector, **P** is the nuclear quadrupole tensor, and μ_N is the nuclear magneton.[14] Although two isotopes of molybdenum have nuclear spins (^{95}Mo (15.7%, $I = 5/2$) and ^{97}-Mo (9.5%, $I = 5/2$)), the remaining isotopes ^{94}Mo + ^{96}Mo + ^{98}-Mo + ^{100}Mo being spin inactive (74.8%, $I = 0$)), no large metal hyperfine coupling (hfc) is resolved. Accordingly, eq 1 was simplified by excluding the nuclear electric quadrupole and nuclear Zeeman interactions. The line widths were assumed to be isotropic (50:50 Lorentzian/Gaussian with a line width of 1 G). The simulated spectrum of Figure 6a was obtained using the following values: $g_x = 2.050$, $g_y = 2.038$, $g_z = 1.990$; ^{31}P hfc, $a_{xx} = a_{yy} = 25$ G, $a_{zz} = 29$ G; ^{1}H hfc, $a_{xx} = a_{yy} = a_{zz} = 5$ G. A ^{95}Mo/^{97}Mo hfc of $a_{xx} = a_{yy} = a_{zz} \approx 1$ G was unresolved but indicated by several peaks that are weighted approximately one-third the height of the main peaks.

Electronic Structure and Geometry Calculations. Electronic structure calculations and geometry optimizations were carried out using a variety of theoretical models. Geometrical conformations of the free TRIPOD molecule were initially explored by both Monte Carlo[15] and molecular dynamics methods (MM2[16] force field) with the BATCHMIN[17] program, and the results were analyzed with the aid of MacroModel.[17] Initial electronic structure calculations were carried out with the aid of SPARTAN 5.0.[18] The SPARTAN package was also used for creation of the orbital and density figures. The geometries of (η^6-C_6H_6)$Mo(CO)_3$, [(η^6-C_6H_6)$Mo(CO)_3$]$^+$, (η^6-C_6H_6)$Mo(PH_3)_3$, and [(η^6-C_6H_6)$Mo(PH_3)_3$]$^+$ were optimized at the pBP/DF* level. The perturbative Becke−Perdew method (pBP) is analogous to the BP method, but the gradient correction is introduced only after convergence based on the local potential alone has been achieved. DN* is a Gaussian basis set similar to 6-31G*, except five pure d-type functions are used instead of six second-order Gaussians.

Following these results, more extensive ab initio and density functional electronic structure calculations for the free TRIPOD molecule and for (η^6-C_6H_6)$Mo(CO)_3$, (η^6-C_6H_6)$Mo(PH_3)_3$, and their positive ions were carried out using the GAUSSIAN 94[19] package of programs. All of these calculations used the LANL2DZ basis set, which is the Dunning−Huzinaga full double-ζ basis for first-row atoms,[20] and the Los Alamos ECP plus DZ on other atoms.[21−23] Partial geometry optimizations of the neutral molecules were carried out by starting from the geometries optimized above and using the B3PW91 model, which is the three-parameter functional of Becke[24] with the nonlocal correlation provided by Perdew and Wang.[25] The results were similar to those obtained above using the pBP/DF* method. Møller−Plesset correlation energy corrections,[26] truncated at second order for MP2,[27−29] were carried out for selected geometries as reported. The potential energy surface for protonation of the model compound (η^6-C_6H_6)$Mo(PH_3)_3$ was investigated using the B3PW91 method. In these calculations,

(9) Lichtenberger, D. L.; Copenhaver, A. S. *J. Electron Spectrosc. Relat. Phenom.* **1990**, *50*, 335.
(10) Chandramouli, G. V. R.; Lalitha, S.; Manoharan, P. T. *Comput. Chem.* **1990**, *14*, 257.
(11) Herring, F. G.; Legzdins, P.; Richter-Addo, G. B. *Organometallics* **1989**, *8*, 1485.
(12) Connelly, N. G.; Geiger, W. E. *Chem. Rev.* **1996**, *96*, 877.
(13) SimFonia, written by Ralph T. Weber, Bruker Instruments, Inc., 1995.
(14) Abragam, A.; Bleaney, B. *Electron Paramagnetic Resonance of Transition Metal Ions*; Clarendon Press: Oxford, U.K., 1970.
(15) Chang, G.; Guida, W. C.; Still, W. C. *J. Am. Chem. Soc.* **1989**, *111*, 4379.
(16) Allinger, N. L. *J. Am. Chem. Soc.* **1977**, *99*, 8127.
(17) Mohamadi, F.; Richards, N. G. J.; Guida, W. C.; Liskamp, R.; Lipton, M.; Caufield, C.; Chang, G.; Hendrickson, T.; Still, W. C. *J. Comput. Chem.* **1990**, *11*, 440.
(18) Spartan Version 5.0; Wavefunction, Inc., 18401 Von Karman Ave., Suite 370, Irvine, CA 92612.
(19) Frisch, M. J.; Trucks, G. W.; Schlegel, H. B.; Gill, W.; Johnson, B. G.; Robb, M. A.; Cheeseman, J. R.; Keith, T.; Petersson, G. A.; Montgomery, J. A.; Raghavachari, K.; Al-Laham, M. A.; Zakrzewski, V. G.; Ortiz, J. V.; Foresman, J. B.; Cioslowski, J.; Stefanov, B. B.; Nanayakkara, A.; Challacombe, M.; Peng, C. Y.; Ayala, P. Y.; Chen, W.; Wong, M. W.; Andres, J. L.; Replogle, E. S.; Gomperts, R.; Martin, R. L.; Fox, D. J.; Binkley, J. S.; Defrees, D. J.; Baker, J.; Stewart, J. P.; Head-Gordon, M.; Gonzalez, C.; Pople, J. A. Gaussian 94, Revision E.2; Gaussian, Inc., Pittsburgh, PA, 1995.
(20) *Methods of Electronic Structure Theory*; Dunning, J. T. H., Hay, P. J., Eds.; Plenum: New York, 1976; pp 1−28.
(21) Hay, P. J.; Wadt, W. R. *J. Chem. Phys.* **1985**, *82*, 299.
(22) Wadt, W. R.; Hay, P. J. *J. Chem. Phys.* **1985**, *82*, 284.
(23) Hay, P. J.; Wadt, W. R. *J. Chem. Phys.* **1985**, *82*, 270.
(24) Becke, A. D. *J. Chem. Phys.* **1993**, *98*, 5648.
(25) Perdew, J. P.; Wang, Y. *Phys. Rev.* **1992**, *B45*, 13244.
(26) Møller, C.; Plesset, M. S. *Phys. Rev.* **1934**, *46*, 618.
(27) Frisch, M. J.; Head-Gordon, M.; Pople, J. A. *Chem. Phys. Lett.* **1990**, *166*, 281.
(28) Frisch, M. J.; Head-Gordon, M.; Pople, J. A. *Chem. Phys. Lett.* **1990**, *166*, 275.
(29) Head-Gordon, M.; Pople, J. A.; Frisch, M. J. *Chem. Phys. Lett.* **1988**, *153*, 503.

Table 1. Analytical Representations of Photoelectron Ionizations and Labels of Primary Characters

compd[a]	position (eV)	width (eV)	rel area He I	rel area He II	label
TRIPOD	7.46	0.46	1.0		P lp
	7.92	0.60			
	8.88	0.87	4.9		Ph π
	10.08	0.53			
	10.54	0.60	9.8		P−C σ
	11.52	1.04			
(Bz)Mo(CO)$_3$	7.43	0.28	1.0		Mo d
	7.65	0.38			
	10.58	0.47	0.8		Bz π
	11.13	0.82			
(Mes)Mo(CO)$_3$	7.16	0.37	1.0	1.0	Mo d
	7.36	0.40			
	9.89	0.35	1.0	0.7	Mes π
	10.25	0.48			
(Bz)Mo(TRIPOD)	5.12	0.38	1.0	1.0	Mo d
	5.37	0.38			
	5.62	0.46			
	7.93	0.38	16.1	9.6	Mo−P σ, Ph π, Bz π
	8.48	0.60			
	8.99	0.86			
	10.08	0.66			
	10.73	0.95	9.4	4.6	P−C σ
	11.44	1.00			

[a] Abbreviations: Bz = (η^6-C_6H_6); Mes = (η^6-1,3,5-$C_6H_3Me_3$).

(η^6-C_6H_6)Mo(PH_3)$_3$ was constrained to C_{3v} symmetry and [(η^6-C_6H_6)Mo(PH_3)$_3$(H)]$^+$ to C_s symmetry. All other geometric parameters were optimized at each point on the path of protonation.

Experimental Results and Discussion

The focus of these studies is the characterization of the energy and electron distribution of the frontier orbitals of (η^6-C_6H_6)Mo(TRIPOD) and characterization of the energy, geometry, and unpaired spin distribution of the lowest positive ion states. The results of computational studies in support of these observations will be discussed subsequently. This information forms the basis for discussion in the final section of the mechanism of protonation of (η^6-C_6H_6)Mo(TRIPOD).

Photoelectron Information. The analytical representations of the photoelectron data and the general assignments of the low-energy valence ionizations are given in Table 1. Assignments of the ionizations are made by comparison of the spectra of these compounds with each other and with spectra of related phosphine and (η^6-arene)M(CO)$_3$ complexes which have been reported previously and which are reproduced here. The label assigned to each ionization corresponds to the predominant metal or ligand character of the orbital from which the ionization arises. The metal d orbital based ionizations are well separated to lower ionization energy from the arene-, phosphine-, phenyl-, and carbonyl-based ionizations of these complexes and are easily identified. Although the labeling of predominant character is useful for the purposes of discussion, the contributions of character from other atoms are important to the ionization energy shifts and are very important to understanding the protonation of these complexes. We will begin by looking at the ionizations of (η^6-arene)M(CO)$_3$ molecules and then consider the ionizations of the free TRIPOD molecule. These molecules provide the basis for interpretation of the ionizations of (η^6-C_6H_6)Mo(TRIPOD).

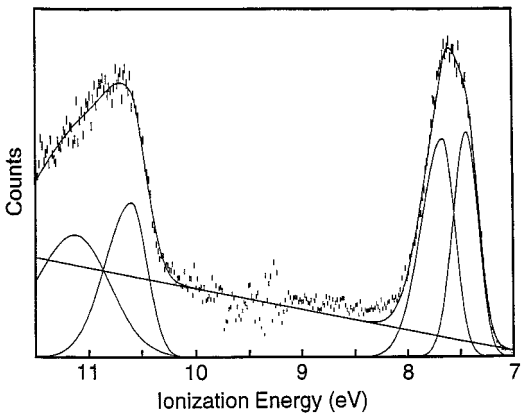

Figure 1. He I photoelectron spectrum of (η^6-C_6H_6)Mo(CO)$_3$.

Photoelectron Spectra of (η^6-arene)M(CO)$_3$ Molecules. The photoelectron spectra of many (η^6-arene)M(CO)$_3$ molecules have been investigated.[30−33] The valence ionizations of the parent derivative, (η^6-C_6H_6)Mo(CO)$_3$, have been discussed previously,[32] but the spectrum was not shown and the specific ionization energies were not listed. For a direct comparison to (η^6-C_6H_6)Mo(TRIPOD), we re-collected the He I spectrum of (η^6-C_6H_6)Mo(CO)$_3$. Some thermal decomposition was observed, and we found it necessary to carry out a spectral subtraction to remove ionizations of free benzene, as has been done previously for other compounds that lose ligands during sublimation.[34] Fortunately, the valence ionizations of free benzene are not in the region of the metal-based ionizations and the spectral subtraction did not affect this region. We found no stability problem with the corresponding mesitylene derivative (η^6-1,3,5-$C_6H_3Me_3$)Mo(CO)$_3$, and the spectrum of this complex, slightly shifted from the spectrum of (η^6-C_6H_6)Mo(CO)$_3$, confirmed the observations for the benzene derivative.

The He I spectrum of (η^6-C_6H_6)Mo(CO)$_3$ is shown in Figure 1. The ionization band at 7−8 eV has been assigned previously to overlap of the ^{2}E and ^{2}A$_1$ ion states, corresponding to removal of electrons from the e and a$_1$ sets of filled metal orbitals descended from the t$_{2g}$ metal orbitals in octahedral symmetry. The use of C_{3v} molecular symmetry for labeling of the ion states is not strictly correct. First, the ^{2}E ion state is expected to split slightly due to Jahn−Teller distortion to lower symmetry, such as seen in the photoelectron spectrum of Fe(CO)$_5$.[35] The expected magnitude of this splitting based on calculations is discussed later. Second, the ^{2}E and ^{2}A$_1$ ion states will mix and split according to the atomic spin−orbit coupling parameter of molybdenum, as seen in the photoelectron spectrum of other second-

(30) Guest, M. F.; Hillier, I. H.; Higginson, B. R.; Lloyd, D. R. *Mol. Phys.* **1975**, *29*, 113.
(31) Gower, M.; Kane-Maguire, L. A.; Maier, J. P.; Sweigart, D. A. *J. Chem. Soc., Dalton Trans.* **1977**, 316.
(32) Byers, B. P.; Hall, M. B. *Organometallics* **1987**, *6*, 2319.
(33) Green, M. L. H.; Hughes, A. K.; Lincoln, P.; Martin-Polo, J. J.; Mountford, P.; Sella, A.; Wong, L.-L.; Bandy, J. A.; Banks, T. W.; Prout, K.; Watkin, D. J. *J. Chem. Soc., Dalton Trans.* **1992**, 2063.
(34) Lichtenberger, D. L.; Sellmann, D.; Fenske, R. F. *J. Organomet. Chem.* **1976**, *117*, 253.
(35) Hubbard, J. L.; Lichtenberger, D. L. *J. Chem. Phys.* **1981**, *75*, 2560.

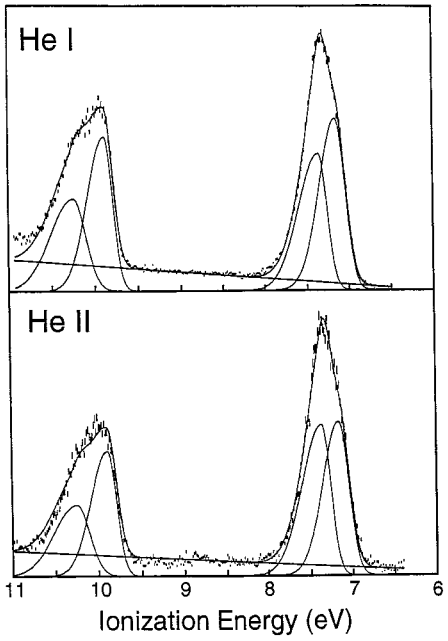

Figure 2. He I and He II photoelectron spectra of (η^6-1,3,5-$C_6H_3Me_3$)$Mo(CO)_3$.

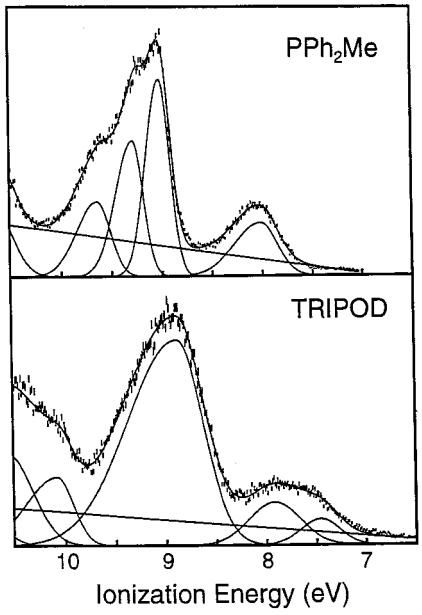

Figure 3. Comparison of the He I photoelectron spectrum of methyldiphenylphosphine with that of the free TRIPOD molecule, 1,1,1-tris((diphenylphosphino)methyl)ethane.

row transition-metal complexes such as ruthenocene,[36] and other piano stool complexes such as $CpRe(CO)_3$.[37] The spin−orbit coupling constant for molybdenum is rather small ($\xi \cong 0.070$ eV), and splitting of the ^2E state due to spin−orbit coupling would be a maximum of 2ξ or about 0.14 eV depending on the metal character of the orbitals. These effects are often negligible compared to the splitting of the metal states caused by electronic interactions with the ligands, but in this case ionizations from the three filled metal-based orbitals are nearly isoenergetic. The energy separation of the positive ion states is less than the width of the vibrational energy progressions, and a definite assignment of the ionizations within the band is not possible. The important point is that the three lowest positive ion states are close in energy.

The band located between 10.5 and 11.5 eV in the spectrum of (η^6-C_6H_6)$Mo(CO)_3$ is assigned to ionization from the predominantly benzene orbitals descended from the e_{2g} π bond orbitals of free benzene. This ionization has been stabilized about 1 eV from the $^2E_{2g}$ ionization of free benzene due to bonding and electron donation from this orbital to the metal.

The valence ionizations of (η^6-1,3,5-$C_6H_3Me_3$)$Mo(CO)_3$ from 6 to 11 eV are shown in Figure 2. The ionizations from the filled metal orbitals can be reasonably represented with two Gaussian peaks at 7.16 and 7.36 eV, while the ionizations associated with the e_{2g} orbital of the mesitylene ligand are modeled with two Gaussian peaks at 9.89 and 10.25 eV. These compare to vertical ionization energies previously reported for (η^6-1,3,5-$C_6H_3Me_3$)$Mo(CO)_3$ of 7.35 eV for the metal ionizations and 10.08 eV for the mesitylene ionizations.[31] The metal ionizations have been destabilized about 0.3 eV and the ligand ionizations have been destabilized about 0.7 eV from those of (η^6-C_6H_6)$Mo(CO)_3$. Comparison of the He I and He II spectra of (η^6-1,3,5-$C_6H_3Me_3$)$Mo(CO)_3$ shows that the ionizations labeled metal-based increase in intensity compared to the mesitylene-based ionizations. This behavior is typically observed for organometallic metal carbonyl complexes,[38] although to a first approximation from theoretical photoionization cross sections of molybdenum and carbon little change is expected.[39] The relative increase in metal-based ionizations observed in the He II spectrum of $Mo(CO)_6$ has been attributed to a resonance enhancement of the metal-based ionizations at ionization energies close to 40 eV.[40]

Photoelectron Spectrum of 1,1,1-Tris((diphenylphosphino)methyl)ethane. In the arene−molybdenum molecule of this study, the tridentate TRIPOD ligand is bound to the metal in place of the three carbonyl ligands in the molecules discussed above. It is instructive to compare the low-energy photoelectron spectrum of the free TRIPOD molecule with that of methyldiphenylphosphine, as shown in Figure 3. The photoelectron spectra of simple alkylphosphine molecules with from one to three phenyl groups bound to the phosphorus atom have been studied previously.[41] The ionizations in the low valence region of the spectra of these phosphines arise from the phosphorus lone pairs and the phenyl π-based orbitals (a_2 and b_1 local symmetry π orbitals on each phenyl group). A filled−filled interaction between the phosphorus lone pair orbital and the phenyl b_1 π orbital spreads the phosphorus lone pair character over two molecular orbitals with ionization energies on either side of the phenyl a_2 orbital ionizations. The lower energy ionization near 8 eV in the spectrum of methyldiphenylphosphine is well-separated from the phenyl a_2 π ionization band near 9 eV and contains the predominant phosphorus lone pair

(36) Lichtenberger, D. L.; Elkadi, Y.; Gruhn, N. E.; Hughes, R. P.; Curnow, O. J.; Zheng, X. *Organometallics* **1997**, *16*, 5209.
(37) Lichtenberger, D. L.; Fenske, R. F. *J. Am. Chem. Soc.* **1976**, *98*, 50.
(38) Green, J. C. *Acc. Chem. Res.* **1994**, *27*, 131−137.
(39) Yeh, J. J.; Lindau, I. *At. Data Nucl. Data Tables* **1985**, *32*, 7.
(40) Cooper, G.; Green, J. C.; Payne, M. P.; Dobson, B. R.; Hillier, I. H. *J. Am. Chem. Soc.* **1987**, *109*, 3836.
(41) Rempe, M. E. *Abstr. Int. B* **1994**, *55*, 1842 (University of Arizona, Tucson, AZ).

character. It is labeled as "P lp", although it should be remembered that there is appreciable mixing with the phenyl b_1 orbital. The high-energy shoulder (9.6 eV) on the phenyl a_2 π ionization band is labeled "phenyl b_1 π", and it shares the phosphorus character.

The TRIPOD molecule consists of three phosphines linked together by alkane bridges. In the absence of interaction between the low valence orbitals of the three phosphines and assuming chemical equivalence, the ionizations of the three linked phosphines will coincide and the photoelectron spectrum of TRIPOD will appear as that of a single phosphine. This is largely the case. The ionizations of TRIPOD are shifted slightly to lower energy from those of methyldiphenylphosphine, because the linking alkane bridge with three connected phosphines is less electronegative than the methyl group of the simple methyldiphenylphosphine. The three phosphorus lone pair based ionizations appear in a band in the region of 7−8.5 eV. Two Gaussian peaks in a roughly 1:2 intensity pattern are necessary to model the profile of this band. The slight splitting of the phosphine lone pair ionizations as indicated by the breadth and the profile of this band suggests either that the phosphine lone pairs are weakly interacting with each other or that the preferred conformation of the free TRIPOD molecule has the phosphines in chemically distinct environments. In contrast, the band with the phenyl b_1 and a_2 π-based ionizations at 9 eV is modeled well with a single Gaussian peak. This band contains 12 phenyl π ionizations, 2 from each of the 6 phenyl groups, but the width of the band is typical of that for a single phosphine, indicating that the phenyl groups are not interacting appreciably with each other. This then implies little direct contact between the phosphorus atoms, because such contact would bring the phenyl groups into close proximity. Both molecular mechanics and ab initio analysis of the TRIPOD molecule conformations, which will be discussed later, support the conclusion of low symmetry for the free TRIPOD molecule with little interaction between the phosphorus atoms and with two distinct chemical sites for the three phosphorus atoms in the preferred conformation. The preferred conformation of the free TRIPOD molecule is most likely not that observed in the tridentate coordination to the molybdenum atom, where the three phosphorus atoms are equivalent and the lone pairs are endodentate.

Photoelectron Spectrum of (η^6-C_6H_6)Mo(TRIPOD). A comparison of the He I spectra of the TRIPOD molecule and (η^6-C_6H_6)Mo(TRIPOD) is shown in Figure 4. In the spectrum of (η^6-C_6H_6)Mo(TRIPOD), the phosphorus lone pair ionizations are stabilized from those of the free molecule by coordination to the metal. The phosphorus lone pair ionizations of phenyl phosphines, including the phenyl b_1 ionization that contains some phosphorus lone pair character, are typically stabilized about 0.8 eV upon coordination to a metal.[42] On the basis of the previous studies of metal−phosphine molecules, the ionization band at 7.93 is associated with the Mo−P σ bonds of (η^6-C_6H_6)Mo(TRIPOD) formed from phosphorus lone pair donation to the metal. This band has nearly merged with the broad and intense ionization band from 8 to 9 eV, which includes both the benzene π and phenyl a_2 ionizations. The ionization at 10.08 eV arises from the phenyl b_1 ionization that has been stabilized away from the phenyl a_2 ionization because of its phosphorus lone pair character interaction with the metal. The ionizations just above 11 eV in the spectra of the ligand and the complex are due to P−C σ bonds.

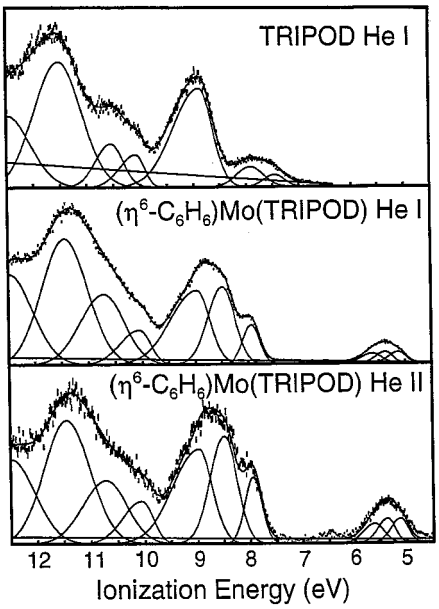

Figure 4. Comparison of the He I photoelectron spectrum of the TRIPOD molecule with the He I and He II photoelectron spectra of (η^6-C_6H_6)Mo(TRIPOD).

The band at 5−6 eV in the spectrum of (η^6-C_6H_6)Mo(TRIPOD) corresponds to the metal-based ionizations. The first ionization of 5.12 eV has been destabilized about 2.3 eV from the metal-based ionizations of (η^6-C_6H_6)$Mo(CO)_3$. This amount of destabilization is expected for the substitution of three carbonyls by three phosphines. For comparison, the first ionization of (η^6-$C_6H_5CH_3$)$Mo(P(CH_3)_3)_3$ is at 5.3 eV.[33] The higher ionization energy for (η^6-$C_6H_5CH_3$)$Mo(P(CH_3)_3)_3$ compared to (η^6-C_6H_6)Mo(TRIPOD), despite the presence of an electron-donating methyl substitution on the arene of (η^6-$C_6H_5CH_3$)$Mo(P(CH_3)_3)_3$, indicates that the TRIPOD ligand is a better donor than the combination of three $P(CH_3)_3$ ligands. This trend may at first appear somewhat surprising, since the TRIPOD ligand bears two phenyl groups per P atom, and a phenyl group is expected to be a poorer donor group than a methyl group (i.e., the pK_b value of a diarylalkylphosphine is typically less than the pK_b value of a trialkylphosphine). However, previous photoelectron studies that compare alkyl and aryl phosphines confirm that the latter are better donors in the gas phase,[43,44] a trend that is attributed to the filled−filled interaction between the phosphorus lone pair electrons and the phenyl b_1 π electrons. Overall, the donor properties of the TRIPOD ligand are exactly as expected for similarly substituted monodentate phosphines, and there is no indication of electronic effects from chelation or strain with coordination. Unlike the case of the (η^6-arene)$Mo(CO)_3$ molecules, where

(42) Bancroft, G. M.; Dignard-Bailey, L.; Puddephatt, R. *Inorg. Chem.* **1986**, *25*, 3675.

(43) Puddephatt, R. J.; Bancroft, G. M.; Chan, T. *Inorg. Chim. Acta* **1983**, *73*, 83.

(44) Puddephatt, R. J.; Dignard-Bailey, L.; Bancroft, G. M. *Inorg. Chim. Acta* **1985**, *96*, L91.

the metal band could be represented by two Gaussian peaks, the detailed shape of the metal band of (η^6-C_6H_6)-Mo(TRIPOD) requires representation by three Gaussian peaks. The need to fit the metal ionization of (η^6-C_6H_6)-Mo(TRIPOD) with three Gaussian peaks is significant because it indicates that the ^{2}E ion state is split to some extent in energy, as discussed above for the tricarbonyl molecules. The Gaussian peaks used to model the metal ionization are separated by 0.24 eV. Spin−orbit splitting of the ^{2}E state would be no more than about 0.14 eV as mentioned previously; therefore, the observed splitting is too large to be attributed solely to spin−orbit coupling. The primary splitting of the ^{2}E state is therefore most likely due to a Jahn−Teller distortion of the degenerate ion state to lower symmetry. This conclusion is also indicated by the rhombic nature of the EPR spectra (vide infra). MO calculations will provide more information regarding this issue.

The He I and He II spectra of (η^6-C_6H_6)Mo(TRIPOD) are compared in Figure 4. The He I and He II spectra of compounds containing phosphorus that have been reported previously, such as $Mo(CO)_5PPh_3$[45] and Cp*Mn-$(PMe_3)_2(CO)$,[46] have shown that predominantly phosphorus-based ionizations decrease in intensity relative to primarily carbon-based and metal-based ionizations. In comparison to the ionizations from 5 to 6 eV, all of the ionizations above 7 eV decrease in relative intensity, as expected due to the spread of ionizations containing phosphorus character throughout this higher energy region. Close examination of Figure 4 also shows that the two Gaussian peaks describing the metal band intensity on the lower energy side increase in the He II spectrum compared to the Gaussian modeling the metal band intensity on the high-energy side. The similar intensity change of the first two peaks modeling the band suggests that the slightly split ^{2}E ionization is associated with the low-energy side of the ionization band. The trend in intensities is reasonable because the a_1 orbital has poor overlap with the arene ligand, while the e orbital overlaps well (vide infra) and is expected to have more carbon character.

Electrochemical Measurements. In CH_2Cl_2 solution, (η^6-C_6H_6)Mo(TRIPOD) exhibits two reversible one-electron oxidation waves at all scan rates, as shown for example in Figure 5. We obtain $E(Mo^{I/0}) = -0.56$ V with $\Delta_p = 99$ mV and $E(Mo^{II/I}) = +0.66$ V with $\Delta_p = 100$ mV versus SCE. The first oxidation potential for (η^6-C_6H_6)-Mo(TRIPOD) is quite low. Perhaps the most relevant comparison with respect to the present paper is the redox potential of (η^6-C_6H_6)$Mo(CO)_3$ versus (η^6-C_6H_6)-Mo(TRIPOD). Unfortunately, (η^6-C_6H_6)$Mo(CO)_3$ does not exhibit reversible oxidation in CH_2Cl_2. It does exhibit quasi-reversible oxidation in $NCCH_3$, but (η^6-C_6H_6)Mo(TRIPOD) is not soluble in $NCCH_3$. Assuming about 100 mV negative shift in the oxidation potential in $NCCH_3$ as compared with CH_2Cl_2,[12] we estimate the Mo^I/Mo^0 couple for (η^6-C_6H_6)Mo(TRIPOD) is roughly 1.5 V more negative than that for (η^6-C_6H_6)$Mo(CO)_3$. Electrochemical and photoionization data generally yield empirical relationships of the form $E_{1/2} =$ (0.6 to 0.8)IP − (3.5 to 4.5).[47−50] Using such a relationship, the difference of 2.4 eV observed for the first ionizations of (η^6-C_6H_6)$Mo(CO)_3$ and (η^6-C_6H_6)Mo(TRIPOD) should correspond to a difference of $E_{1/2}$ in the range of 1.4−1.9 V. The good agreement with this expectation indicates that the trends observed from the gas-phase measurements are relevant to the solution-phase properties.

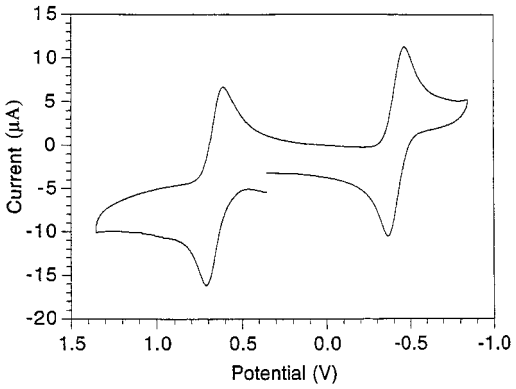

Figure 5. Cyclic voltammogram (V vs SCE) of (η^6-C_6H_6)-Mo(TRIPOD).

Electron Paramagnetic Resonance Spectra. The X-band EPR spectrum of [(η^6-C_6H_6)Mo(TRIPOD)]$^+$ is presented in Figure 6a. An EPR signal was observed only at temperatures below 25 K. A first-harmonic Q-band spectrum of [(η^6-C_6D_6)Mo(TRIPOD)]$^+$ that reveals the nonisotropic nature of the EPR spectra is illustrated in Figure 6c. The second harmonic of the Q-band spectrum of [(η^6-C_6D_6)Mo(TRIPOD)]$^+$ clearly indicates rhombic symmetry (Figure 6d). Using the *g* factors and the ^{31}P *a* values that were measured from the second-harmonic Q-band spectrum of [(η^6-C_6D_6)Mo-(TRIPOD)]$^+$ (Figure 6d) and ^{1}H *a* values from the first-harmonic X-band spectrum of [(η^6-C_6H_6)Mo(TRIPOD)]$^+$ (Figure 6a), we obtained the simulated spectrum of Figure 6a.

Seventeen-electron organometallics have attracted considerable attention.[51] The EPR spectra of cyclopentadienyl derivatives of group 6 metals have been particularly well studied.[52−54] A few [(η^6-arene)ML_3]$^+$ derivatives have been synthesized and studied by EPR.[55,56] Two distinctive hfc's are observed in the spectrum of [(η^6-C_6H_6)Mo(TRIPOD)]$^+$. The larger hfc of $a_{xx} = a_{yy} =$ 25 G, $a_{zz} = 29$ G is assigned to three ^{31}P nuclei, as suggested by the quartets that are observed in the second harmonic of the Q-band spectrum of [(η^6-C_6D_6)-Mo(TRIPOD)]$^+$ (Figure 6d). An *a* value of 25−30 G is

(45) Rempe, M. E. *Abstr. Int. B* **1994**, *55*, 1842 (University of Arizona, Tucson, AZ).
(46) Lichtenberger, D. L.; Kellogg, G. E. *Acc. Chem. Res.* **1987**, *20*, 379−387.
(47) Morris, R. H.; Earl, K. A.; Luck, R. L.; Lazarowych, N. J.; Sella, A. *Inorg. Chem.* **1987**, *26*, 2674.
(48) Loutfy, R. O. *J. Chem. Phys.* **1977**, *66*, 4781.
(49) Pysh, E. S.; Yang, N. C. *J. Am. Chem. Soc.* **1963**, *85*, 2124.
(50) Howell, J. O.; Goncalves, J. M.; Amatore, C.; Klasinc, L.; Wightman, R. M.; Kochi, J. K. *J. Am. Chem. Soc.* **1984**, *106*, 3968.
(51) Baird, M. C. *Chem. Rev.* **1988**, *88*, 1217.
(52) Krusic, P. J.; McLain, S. J.; Morton, J. R.; Preston, K. F.; LePage, Y. *J. Magn. Reson.* **1987**, *74*, 72.
(53) Morton, J. R.; Preston, K. F.; Cooley, N. A.; Baird, M. C. *J. Chem. Soc., Faraday Trans. 1* **1987**, *83*, 3535.
(54) Fortier, S.; Baird, M. C.; Preston, K. F.; Morton, J. R.; Ziegler, T.; Jaeger, T. J.; Watkins, W. C.; MacNeil, J. H.; Watson, K. A.; Hensel, K.; Page, Y. L.; Charland, J.-P.; Williams, A. J. *J. Am. Chem. Soc.* **1991**, *113*, 542.
(55) VanOrder, N.; Geiger, W. E.; Bitterwolf, T. E.; Rheingold, A. L. *J. Am. Chem. Soc.* **1987**, *109*, 5680.
(56) Connelly, N. G.; Demidowicz, Z.; Kelly, R. L. *J. Chem. Soc., Dalton Trans.* **1975**, 2335.

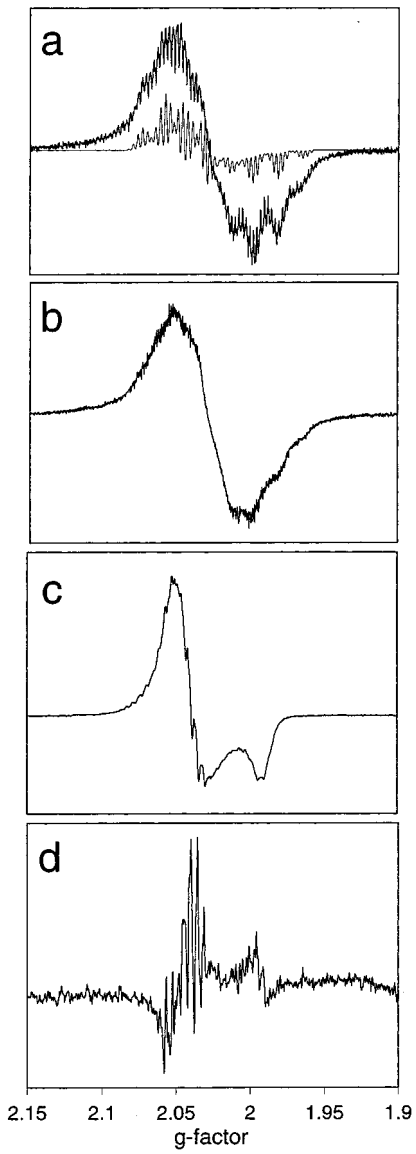

Figure 6. (a) X-band EPR spectrum of $[(\eta^6\text{-}C_6H_6)Mo(TRIPOD)]^+$ at 4 K in THF and a simulation (inset). (b) X-band EPR spectrum of $[(\eta^6\text{-}C_6D_6)Mo(TRIPOD)]^+$ at 4 K in THF. (c) First-harmonic Q-band EPR spectrum of $[(\eta^6\text{-}C_6D_6)Mo(TRIPOD)]^+$ at 50 K in THF. (d) Second-harmonic Q-band EPR spectrum of $[(\eta^6\text{-}C_6D_6)Mo(TRIPOD)]^+$ at 50 K in THF.

typical for ^{31}P hfc in related organometallic metal−phosphorus compounds.[57,58] The smaller ^1H hfc of 5 G is comparable to the 3.8 G *a* value that has been observed for the benzene cation radical[59] and 6.4 G that is observed for the benzene anion radical.[60] This interpretation is supported by the X-band EPR spectrum of the corresponding deuterio isotopomer $[(\eta^6\text{-}C_6D_6)Mo(TRIPOD)]^+$, which is shown in Figure 6b. A similar approach of isotopic substitution has been taken recently in the EPR characterization of some 17-electron cyclopentadienylmolybdenum hydrides.[58] Although a significant difference between the largest *a* values of $[(\eta^6\text{-}C_6H_6)Mo(TRIPOD)]^+$ and $[(\eta^6\text{-}C_6D_6)Mo(TRIPOD)]^+$ is observed, the hfc of $a_{zz} = 27$ G that is observed for $[(\eta^6\text{-}C_6D_6)Mo(TRIPOD)]^+$ is substantially larger than the value of 9 G one would expect from the ratios of the magnetic moments of the hydrogen isotopomers ($(\mu_N(^2H)/\mu_N(^1H) = 0.86/2.79 = 0.31$).[61]

The ^1H hfc observed in the EPR spectrum of $(\eta^6\text{-}C_6H_6)Mo(TRIPOD)]^+$ is particularly significant. The *a* values observed for the π cation and anion radicals of aromatic organic compounds are typically 4−6 G. This coupling has been attributed to $\sigma-\pi$ spin polarization.[62] Although the magnitude of hfc for transition-metal complexes is not simply related to the amount of orbital character,[63,64] proton hfc via spin-polarization is only probable if there is significant benzene π character in the singly occupied molecular orbital (SOMO). Therefore, the arene proton hfc that is observed for $[(\eta^6\text{-}C_6H_6)Mo(TRIPOD)]^+$ indicates that the SOMO of this molecule has substantial arene character. The $^2A_1$ positive ion state is largely metal d_{z^2} in character, and this orbital is essentially orthogonal to the π system of the arene ligand. The ^2E ion state, on the other hand, contains $d_{x^2-y^2}$ and d_{xy} character that is appropriate for back-bonding interaction with the arene π orbitals. Accordingly, the EPR spectra indicate that SOMO of $[(\eta^6\text{-}C_6H_6)Mo(TRIPOD)]^+$ is derived from the e set and the observed rhombic character of the EPR spectra is consistent with the Jahn−Teller distortion that is also indicated by the photoelectron spectroscopy and by the molecular orbital calculations.

Computational Results and Discussion

As with the experiments, the calculations will focus on the structures and frontier orbitals of the $(\eta^6\text{-}C_6H_6)Mo(CO)_3$ and $(\eta^6\text{-}C_6H_6)Mo(TRIPOD)$ molecules, and on the structures, energies, and electron distributions of the lowest positive ion states. The $(\eta^6\text{-}C_6H_6)Mo(CO)_3$ molecule is sufficiently small to allow theoretical computation at a level that corresponds closely to the experiments and provides a good foundation for this study. The replacement of the three carbonyl ligands with the TRIPOD ligand, including its six phenyl groups, greatly increases the size of the calculations. We will investigate the free TRIPOD molecule on its own and model the $(\eta^6\text{-}C_6H_6)Mo(TRIPOD)$ molecule with $(\eta^6\text{-}C_6H_6)Mo(PH_3)_3$.

$(\eta^6\text{-}C_6H_6)Mo(CO)_3$. Table 2 compares the crystal structure geometry of $(\eta^6\text{-}C_6H_6)Mo(CO)_3$ with the geometry that was optimized using the density functional method. The density functional method provides bond distances that are within 0.04 Å and angles that are within 1° of those in the experimental structure.[65] The ab initio Hartree−Fock calculation also agrees well with the experimental bond distances and angles except that

(57) Aston, G. M.; Badriya, S.; Farley, R. D.; Grime, R. W.; Ledger, S. J.; Mabbs, F. E.; McInnes, E. J. L.; Morris, H. W.; Ricalton, A.; Rowlands, C. C.; Wagner, K.; Whiteley, M. W. *J. Chem. Soc., Dalton Trans.* **1999**, 4379.
(58) Pleune, B.; Poli, R.; Fettinger, J. C. *J. Am. Chem. Soc.* **1998**, *120*, 3257.
(59) Feldman, V. I.; Sukhov, F. F.; Orlov, A. Y. *Chem. Phys. Lett.* **1999**, *300*, 713.
(60) Atkins, P. *Physical Chemistry*, 5th ed.; W. H. Freeman: New York, 1994.
(61) Kadam, R. M.; Itagaki, Y.; Benetis, N. P.; Lund, A.; Erickson, R.; Huber, M.; Hilczer, W. *Phys. Chem. Chem. Phys.* **1999**, *1*, 4967.
(62) Gerson, F. *High Resolution E.S.R. Spectroscopy*; Verlag Chemie: Weinheim, Germany, 1970.
(63) Braden, D. A.; Tyler, D. R. *J. Am. Chem. Soc.* **1998**, *120*, 942.
(64) Braden, D. A.; Tyler, D. R. *Organometallics* **1998**, *17*, 4060−4064.
(65) Burgi, H.-B.; Raselli, A.; Braga, D.; Grepioni, F. *Acta Crystallogr., Sect. B* **1992**, *48*, 428.

Table 2. Selected Experimental and Calculated Interatomic Distances (Å) and Angles (deg) for (η^6-C_6H_6)MoL_3[a]

	(η^6-C_6H_6)$Mo(CO)_3$			(η^6-C_6H_6)$Mo(PH_3)_3$		
	exptl[c]	DFT	DFT[d,e]	exptl[c]	DFT	DFT[e]
Mo−C_6[b]	1.91	1.95	1.98	1.82	1.84	1.84
C−C(arene)$_{av}$	1.41(1)	1.43	1.42	1.41(1)	1.43	1.43
Mo−C(arene)$_{av}$	2.38(1)	2.41	2.43	2.30(2)	2.33	2.33
Mo−L	1.961(1)	2.00	2 × 2.04 2.02	2.39(1)	2.41	2.48
C_6[a]−Mo−L	127(2)	128	2 × 129 121	130(1)	128	124
L−Mo−L	87(1)	87	2 × 82 96	84(1)	87	92

[a] All compounds have a symmetry of C_{3v} and a charge of 0 unless otherwise noted. [b] Averaged center of arene ring. [c] Average crystal geometric parameters (and standard deviations from 3-fold symmetry). [d] C_s symmetry. [e] Charge of 1+.

Table 3. Modeled Vertical Ionization Energies (eV) to Lowest Positive Ion States of (η^6-C_6H_6)ML_3

		(η^6-C_6H_6)-$Mo(CO)_3$		(η^6-C_6H_6)-$Mo(PH_3)_3$	
	method	$^2A_1$	^2E	$^2A_1$	^2E
HF	orbital energy	8.45	7.75	6.88	5.88
HF	E(ion)−E(neutral)	6.33	5.97	4.15	3.98
MP2	E(ion)−E(neutral)	7.41	7.40	5.47	5.79
exptl		7.43−7.65		5.12−5.42	

it places the arene ring 0.2 Å too far from the molybdenum center.

Table 3 summarizes the calculated metal-based orbital energies and vertical ionization energies at the optimized geometry. The calculations account very well for the ionization energies obtained from experiment, with the values calculated at the MP2 level of approximation correct within the observed bandwidth of the ionizations. The metal-based e symmetry orbitals are the HOMOs, which are followed closely by the metal-based a_1 symmetry orbital. Earlier extended Hückel molecular orbital calculations predicted the opposite ordering.[66] Estimation of the correlation energies to the second-order level (MP2) is unable to determine definitively whether the ^2E or the $^2A_1$ state is the ground state of the ion when constrained to the C_{3v} geometry of the neutral molecule. The primary point is that, just as observed in the photoelectron spectrum, the energies of these ion states are similar. The electron distributions of these two orbitals are somewhat different. Figure 7 shows that the e symmetry orbitals have more density on the arene ring than the a symmetry orbital.

[(η^6-C_6H_6)$Mo(CO)_3$]$^+$. The molecular structure of [(η^6-C_6H_6)$Mo(CO)_3$]$^+$ as obtained from the calculations indicates changes in geometry that occur from the neutral molecule to the positive ion. The lengthening of the Mo−CO distance and shortening of the C−O distance are qualitatively as expected for the reduced back-bonding from the metal to the carbonyl π^* orbitals in the positive ion. The [(η^6-C_6H_6)$Mo(CO)_3$]$^+$ ion is highly distorted from the C_{3v} symmetry that is typically observed for (η^6-C_6H_6)ML_3 complexes. The major feature of the distortion in the positive ion is an opening of one OC−Mo−CO angle to reduce the symmetry to C_s.

(66) Mailvaganam, B.; Sayer, B. G.; McGlinchey, M. J. *Organometallics* **1990**, *9*, 1089.

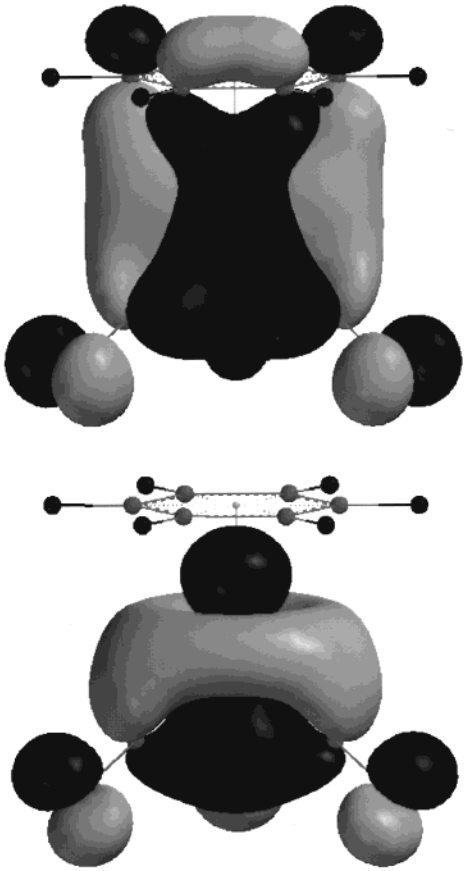

Figure 7. Frontier molecular orbitals of (η^6-C_6H_6)$Mo(CO)_3$ as calculated by the SPARTAN pBP-DF* method. The HOMO (top) of e symmetry has substantial arene character (49% Mo, 19% arene and 32% CO). The SHOMO (bottom) of a_1 symmetry has more metal character (62% Mo, 11% arene and 27% CO). The isodensity surface (0.002 e/au^3) for each diagram is chosen to emphasize the greater delocalization of the e symmetry orbital to the arene ring.

Unfortunately, there are no crystal structures of d^5 (η^6-C_6H_6)$M(CO)_3$ complexes for comparison. Similar distortion has been computed for the d^5 complex (η^5-C_5H_5)-$Cr(CO)_3$.[54] Figure 8 illustrates the dependence of the molecular and orbital energies on the distortion. The distortion of Figure 8 is defined as the torsion angle (γ) that is formed by the unique Mo−C′O bond and one of the symmetry-related Mo−CO bonds about the vector formed by the Mo and the centroid of the arene ligand:

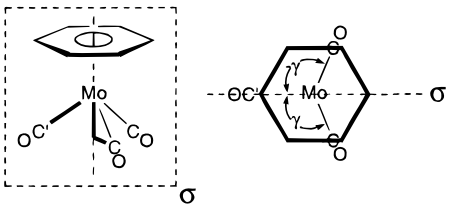

The distortion follows from the Jahn−Teller effect to reduce the degeneracy of a ^2E state in C_{3v} symmetry to $^2A'$ and $^2A''$ states in C_s symmetry.[52,53] The critical factor is the sensitivity of the a′ and a″ orbital energies to the distortion. This case is similar to the example of Jahn−Teller distortion that has been observed in the $^2E''$ ionization of $Fe(CO)_5$.[35] In both cases the carbonyls have some filled−filled σ interaction with the $d_{x^2-y^2}$ and d_{xy} metal orbitals. Removal of electron density from one of

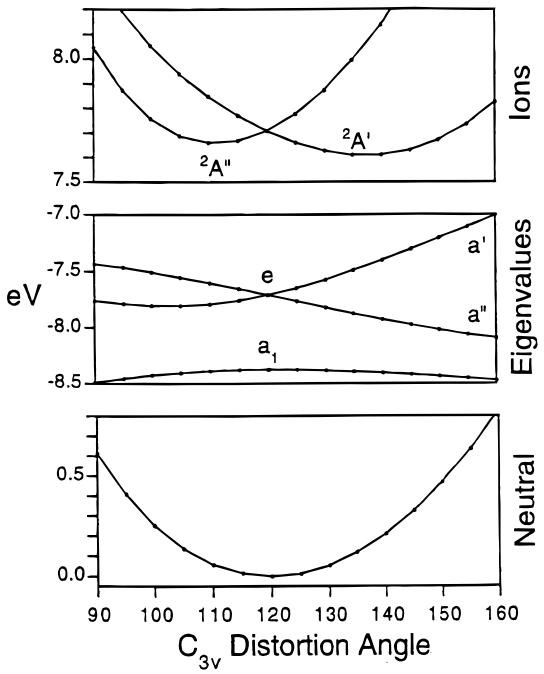

Figure 8. Energy dependence on the distortion of (η^6-C_6H_6)Mo(CO)$_3$ from C_{3v} to C_s symmetry. The distortion angle is defined as the torsion angle that is formed by the unique Mo−CO bond and one of the symmetry-related Mo−CO bonds about the Mo−centroid vector (see text figure). The bottom curve is the restricted Hartree−Fock energy of the neutral molecule relative to the ground-state geometry, the middle curves are the metal-based orbital energies of the neutral molecule, and the top curves are the energies of the positive ions before electron relaxation relative to the neutral ground-state geometry.

these orbitals allows the carbonyls to shift their σ donor orbitals away from the filled metal orbital and toward the metal electron vacancy. Carbonyl π bonding effects also play a role, as illustrated for removal of an electron from the 2a′ orbital:

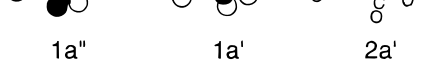

The energy effect for Fe(CO)$_5$ is larger than for the present case, because the metal orbitals of Fe(CO)$_5$ are more purely $d_{x^2-y^2}$ and d_{xy} in character and because the carbonyls are directly in the $x-y$ orbital plane.

The geometric relaxation energy of the ^{2}E positive ion from the geometry of the neutral molecule is about 10 kcal/mol by the density functional method and 22 kcal/mol by the ab initio Hartree−Fock method. Correlation energy corrections to the Hartree−Fock energies significantly reduce the energy associated with geometry optimization of the positive ion.

1,1,1-Tris((diphenylphosphino)methyl)ethane. The photoelectron ionizations indicate that there is little interaction between the three linked phosphines in the free TRIPOD molecule and that two of the phosphine lone pair ionizations are slightly different from the third. Conformational analysis of the TRIPOD molecule yields a large number of structures within 10 kcal/mol of the most stable structure. Many of these structures differ only by slight adjustments to the orientations of the phenyl rings and phosphines. The structures may be grouped according to the general conformations of the phosphines with respect to the ethane bridge. When the TRIPOD ligand is coordinated to the Mo center, each phosphine is in an *anti* conformation with respect to the ethane bridge and each phosphine lone pair points toward the metal. The other conformations are grouped according to one, two, or all three phosphines in *gauche* orientations with respect to the ethane bridge. The most stable conformation from this analysis places two of the phosphines in *gauche* positions, which is consistent with the photoelectron spectrum. Regardless of the particular ground-state conformation, the TRIPOD molecule is sufficiently flexible to adapt to different coordinating environments.

(η^6-C_6H_6)Mo(PH_3)$_3$. The computed molecular structure of (η^6-C_6H_6)Mo(PH_3)$_3$ gives bond distances that are within 0.03 Å and angles that are within 3° of the crystal structure of (η^6-C_6H_6)Mo(TRIPOD).[3] The computed distances of Mo−C(arene)$_{av}$ = 2.33 Å and Mo−P = 2.41 Å are comparable with the distances of Mo−C(arene)$_{av}$ = 2.29 Å and Mo−P = 2.42 Å which have been determined for several (η^6-arene)Mo(phosphine)$_3$ complexes that bear a variety of phosphine ligands.[3,67,68] The structure from the Hartree−Fock calculation is also reasonable except for the Mo−P distance, which is 0.2 Å too long.

The calculated metal-based ionization energies are listed in Table 3. The agreement with the experimental values is excellent again, especially considering the substitution of the TRIPOD ligand by three PH_3 ligands. The experimental first ionization of (η^6-C_6H_6)Mo(TRIPOD) is shifted 2.3 eV to lower energy from that of (η^6-C_6H_6)Mo(CO)$_3$. The calculations listed in Table 3 show shifts of 1.5−2.0 eV. It is clear that the TRIPOD ligand makes the metal very electron rich. The density functional calculations predict about 33% total arene character (primarily derived from the arene e_{2u} orbital) in the predominantly metal e orbital for the model complex (η^6-C_6H_6)Mo(PH_3)$_3$. Because the TRIPOD ligand is expected to be a better donor than PH_3, even more arene character would be expected in this orbital of the TRIPOD complex.

[(η^6-C_6H_6)Mo(PH_3)$_3$]$^+$. The ^{2}E state of [(η^6-C_6H_6)Mo(PH_3)$_3$]$^+$ is subject to Jahn−Teller distortion just as the similar state of the tricarbonyl molecule. The dependence of the orbital and molecular energies on the opening of one P−Mo−P angle is similar to that shown in Figure 8 for the tricarbonyl molecule. The energy dependence is smaller in this case compared to the tricarbonyl, as expected for the longer Mo−P bond lengths and the weaker π acceptance ability of phosphines. The net stabilization with opening of the P−Mo−P angle is about half that observed for the tricarbonyl molecule. In contrast to the corresponding carbonyl derivative, density functional calculations slightly favor a $^2A_1$ ground state for the positive ion in the gas phase which maintains C_{3v} symmetry, and the

(67) Mason, R.; Thomas, K. M.; Heath, G. A. *J. Organomet. Chem.* **1975**, *90*, 195.
(68) Morris, R. H.; Sawyer, J. F.; Sella, A. *Acta Crystallogr., Sect. C* **1988**, *44*, 23.

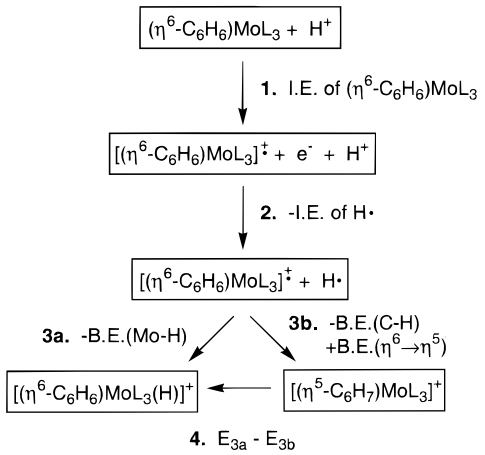

Figure 9. Thermodynamic steps of protonation of (η^6-C_6H_6)MoL_3 in terms of ionization energies (IE) and bond energies (BE). Negative signs indicate stabilization processes. Mo and C denote the molybdenum and arene carbon atoms of the molecule.

geometry stabilization is primarily due to optimization of the Mo−P bond lengths and opening of the Mo−P_3 base. The MP2 corrections to the Hartree−Fock results tend to agree with the density functional calculations, although again the energy differences are small. The $^2A_1$ and ^2E states appear to be close in energy for [(η^6-C_6H_6)Mo(phosphine)$_3$]$^+$ compounds. The photoelectron and EPR results suggest the ground state for [(η^6-C_6H_6)-Mo(TRIPOD)]$^+$ is derived from the E state and Jahn−Teller distortion is indicated.

Mechanism of Protonation

Electrons in the frontier orbitals of a molecule are the most readily available for oxidation and stabilization by way of formation of a two-electron bond with an incoming proton. Frontier orbital control of protonation of organic compounds has been proposed previously.[69] Furthermore, nucleophilic attack on some organotransition-metal complexes is believed to take place under frontier orbital control.[70] For (η^6-arene)$Mo(CO)_3$ and the (η^6-arene)Mo(phosphine)$_3$ derivatives, the highest occupied frontier orbitals are shown by both experiments and calculations to be the predominantly metal a_1 and e orbitals (C_{3v} symmetry) and are close in energy. The a_1 orbital is largely localized on the metal, while the e orbital is partly delocalized onto the arene ligand, and more so for the phosphine derivatives.

A more precise and quantitative description of protonation is provided by the thermodynamics of a stepwise path involving ionization energies and homolytic bond energies as mentioned in the Introduction and shown in more detail for this particular case in Figure 9. This figure underscores the importance of characterizing the energies and electron distributions of the positive molecular ions. The first energy contribution to protonation is ionization of the molecule to create the molecular radical cation and a free electron. The energy of this step is measured directly in the gas phase for these molecules by photoelectron spectroscopy, and the solution electrochemical measurements show that the trends observed in the gas phase remain valid with solvation (vide supra). The second energy step is addition of the electron to the proton. This stabilization energy is 13.6 eV. This step is the primary driving force in terms of energy for protonation of the molecule. The combination of steps 1 and 2, which is simply charge transfer from the molecule to the proton, can occur before full formation of the bond with the hydrogen atom. The most favorable energy for steps 1 and 2 corresponds to the lowest energy positive ion. Because the lowest energy positive ions correspond to ionizations from the highest occupied molecular orbitals, the focus of attention is on these frontier orbitals.

The molecular ion and the hydrogen atom resulting from the electron transfer of steps 1 and 2 are both radicals, and the next step is joining the two to form the electron pair bond. The experiments show that the unpaired electron of the first molecular radical ion is localized largely on the metal with some delocalization to the arene ring. Step 3a in Figure 9 shows direct formation of the Mo−H bond. Step 3b shows formation of the *exo* C−H bond. In the early stages of formation this is not a typical C−H bond because the carbon atom is able to donate only a portion of an unpaired electron to the bond. A larger portion of unpaired density would be available if the molecular ion state from step 1 corresponded to removal of an electron from a benzene based orbital, but the photoelectron spectroscopy shows that this state requires 3 eV of additional energy. In the latter stages of protonation of the arene the C−H bond becomes more normal, but this stabilization is partly compensated by weakening the bonding of the ring to the metal from η^6 to η^5. Overall, the energy along a path of protonation to formation of the electron pair bond is dictated first by the ionization energy to produce the molecular positive ion and second by the access of the hydrogen atom to the unpaired electron density in this molecular ion.

Protonation of (η^6-arene)$Mo(CO)_3$. The thermodynamic product of protonation of (η^6-C_6H_6)$Mo(CO)_3$ places the proton near the $x-y$ plane, consistent with the lower ionization energy of the e symmetry orbitals in this plane. However, since the e and a_1 electrons are both accessible energetically, under certain conditions protonation may occur at the a_1 orbital along the z axis. An earlier EHMO study of (η^6-C_6H_6)$Mo(CO)_3$ supports this idea. This calculation suggested that for sterically demanding arene ligands (e.g., C_6Et_6) electrophilic attack is preferred along the z axis opposite from the arene ligand to give a metal-hydride complex of C_{3v} symmetry.[66] For (η^6-C_6H_6)$Mo(CO)_3$, the metal-based e orbital contains less arene character than the phosphine derivatives because poor energy matching does not allow sufficient mixing with the high-energy lowest unoccupied molecular orbital of the arene, and additional rehybridization occurs at the metal to maximize π overlap of the metal orbitals with the CO ligands. Accordingly, protonation of the arene ligand is not expected to be as favorable for (η^6-arene)$Mo(CO)_3$ compared with (η^6-arene)Mo(phosphine)$_3$ (vide supra).

Protonation of (η^6-arene)Mo(phosphine)$_3$. When the carbonyls are replaced by phosphines, the filled metal orbitals are destabilized by the greater charge

(69) DeKock, R. L. *J. Am. Chem. Soc.* **1975**, *97*, 5592.
(70) Block, T. F.; Fenske, R. F.; Casey, C. P. *J. Am. Chem. Soc.* **1976**, *98*, 441.

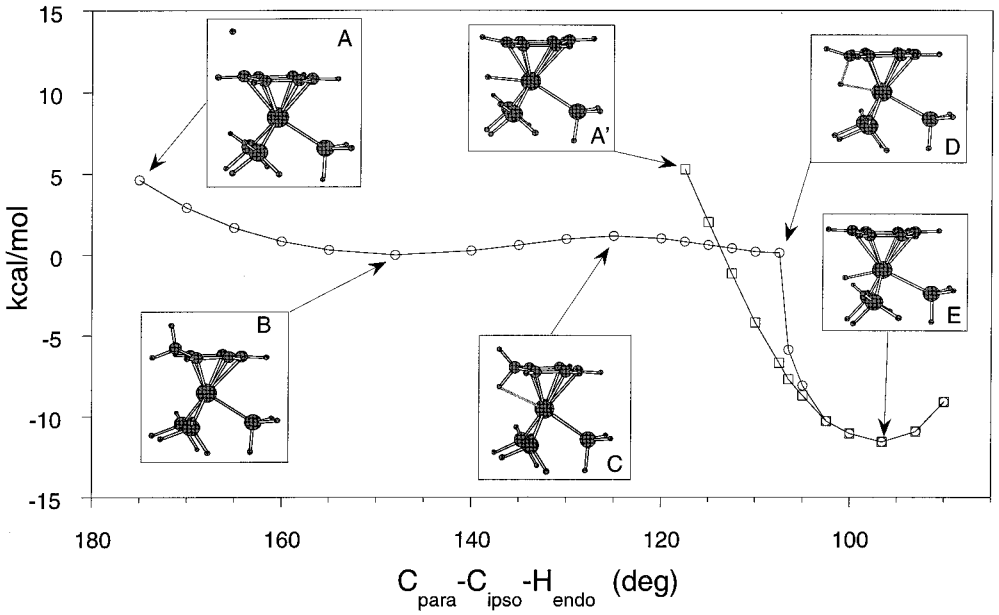

Figure 10. Intrinsic reaction coordinate diagram for the protonation of (η^6-C_6H_6)Mo(PH_3)$_3$ via direct attack on the metal (□, A′ → E) and indirect attack via a cyclohexadienyl transient (○, A → B → C → D → E). Note both pathways converge at C_{para}−C_{ipso}−H ≈ 105°.

potential at the metal center due to the good σ-donor ability of the phosphine as well as loss of π back-bonding. The result is better overlap and energy matching of the e metal orbital with the arene e_{2u} and therefore a substantial amount of arene character in this orbital. The low ionization energy and partial arene character of this frontier orbital enhances protonation at the arene ligand.

Because the theoretical calculations reported herein successfully reproduce the structures of these molecules and the relative energies of the positive ion states, it is worth using them to examine the molecular structures and energies along different paths of the potential surface for protonation. The intrinsic reaction coordinates for gas-phase protonation of the model compound (η^6-C_6H_6)Mo(PH_3)$_3$ are illustrated in Figure 10. Before proceeding with this line of discussion, we must emphasize that these calculations ignore the effects of solvent and the conjugate base of the acid. There are two different "grooves" in the potential energy surface that lead to protonation of the metal, corresponding to direct attack on the metal and indirect attack via protonation of the arene to form the cyclohexadienyl transient. A convenient measurement of the reaction coordinate is the H−C_{ipso}−C_{para} angle, where H is the incoming proton in the case of direct attack on the metal (left) and the *endo* proton in the case of arene attack (right):

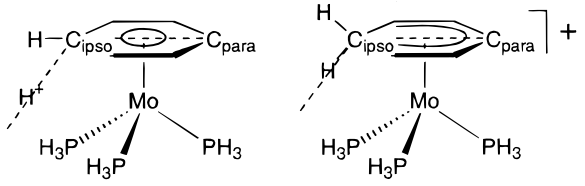

These two pathways join at an angle of about 105°.

Before complete bonding between the proton and the molecule occurs (point A in Figure 10), the arene ring is nearly planar. Oxidation of the molecule has already taken place at this point through electron transfer to the proton. The high driving force for this electron transfer comes from the strong electron attraction to the proton (13.6 eV) compared to the molecular ion (5.1 eV) and the comparative long-range interaction of the coulomb force. At point B, formation of the C−H bond between the proton and the arene creates a coordinated cyclohexadienyl ligand with a geometry that is similar to that of other (η^5-cyclohexadienyl)metal complexes.[71] Note that the carbon of the CH_2 group has nearly sp^3 geometry and it is bent up out of the plane of the rest of ring. This carbon is no longer bonding to the metal, and the hydrogens on this carbon are too far from the metal for direct interaction with the metal. Unlike most other such η^5-cyclohexadienyl complexes, this is a 16-electron metal complex with a +II, d^4 metal center (considering the +1 charge on the complex and the formal −1 charge of the cyclohexadienyl ligand). The calculations show that the electron charge flow to the new C−H bond comes from the metal and the phosphines. Point C, the transition state that brings the *endo* C−H bond to the metal to satisfy the electron deficiency, requires only about 2 kcal/mol from the minimum of the η^5-cyclohexadienyl well in these calculations. The transition state occurs when the carbons of the ring are again nearly planar. The formation of the Mo−H bond (starting from point D) lowers the energy dramatically and quickly breaks the C−H bond. This is the region in which the potential curve for protonation facilitated by

(71) An example is the crystal structure of (η^5-1,2,4,6-tetramethylhexadienyl)Mn(CO)$_3$ (Gaudet, M. V.; Hanson, A. W.; White, P. S.; Zaworotko, M. J. *Organometallics* **1989**, *8*, 286). Crystal structures of (η^5-cyclohexadienyl)metal complexes show the five unsaturated carbon atoms of the cyclohexadienyl ring bound to the metal center and the single sp^3 carbon atom of the ring bent up from the C_5 plane. The angle between the C_5 plane and the C_3 plane containing the sp^3 carbon atom is typically near 40°. A calculation of the geometry of this Mn complex using the same method as for the structures in Figure 10 reproduces the experimental bond lengths within an average of 0.02 Å and reproduces the experimental bond angles with an average of less than 1°, including the angle of the sp^3 carbon atom from the C_5 plane. The angle of the sp^3 carbon atom from the C_5 plane for structure B of (η^5-C_6H_7)Mo(PH_3)$_3$ in Figure 10 is 28°.

the arene joins the potential curve for direct Mo−H formation (curve A′ ⇌ E).

Protonation of (η^6-arene)Mo(TRIPOD). The TRIPOD ligand imposes unusual properties on the metal center of (η^6-C_6H_6)Mo(TRIPOD). By comparison with analogous monodentate ligands, chelating phosphines are likely to raise the barriers of associative reactions by adding strain energy to the geometric distortions that occur with expansion of the coordination number of the metal. Bulky phosphines also add steric constraints to the approach of a ligand. The TRIPOD ligand, while rendering the metal center very electron-rich, also encapsulates the metal center, sterically protecting it from direct attack by electrophiles. The area of the a_1 orbital along the *z* axis is protected by the ethane linkage of the TRIPOD ligand. Furthermore, the portions of the e symmetry orbitals along the *x*−*y* plane are protected by the phenyl groups of the TRIPOD ligand. Since the proton is delivered as a tight ion pair with its conjugate base in nonpolar solvents such as CH_2Cl_2, protonation is unable to take place directly at the metal. The initial step in the mechanism therefore involves electrophilic attack at the most kinetically accessible site of frontier orbital electron density. This study of the electronic structure of (η^6-C_6H_6)Mo(TRIPOD) demonstrates that while the frontier electron density is primarily metal in character, there is also a sizable amount of arene character. The arene character provides a kinetically accessible site for electrophilic attack, thereby allowing the thermodynamic product to be formed eventually.

In conclusion, indirect proton attack at the *exo* position of the arene does not involve a different frontier orbital than direct attack on the metal center but, instead, involves a different portion of the same molecular orbital. The necessary conditions for the arene mechanism of protonation displayed by (η^6-C_6H_6)Mo(TRIPOD) include (1) a highly electron rich metal center, (2) arene character in the highest occupied orbital, and (3) steric protection of the metal. We have recently reported experimental evidence that other phosphine derivatives are protonated directly at the metal if the phosphines do not provide sufficient steric protection.[72]

Acknowledgment. M.T.A. thanks the National Science Foundation (Grant No. CHE-9612869) and the Oklahoma Center for the Advancement of Science and Technology (OCAST HR98-078) for their financial support. The EPR instrument used in this study was also financed by the National Science Foundation (Grant No. CHE-9512996). D.L.L. acknowledges support by the U.S. Department of Energy (Division of Chemical Sciences, Office of Basic Energy Sciences, Office of Energy Research, Contract No. DE-FG03-95ER14574), the National Science Foundation (Grant No. CHE-9618900), and the Materials Characterization Program, Department of Chemistry, University of Arizona. We thank Dr. Ralph T. Weber for his assistance with the Q-band EPR experiment and the reviewers of this paper for helpful suggestions.

OM990673U

(72) Ashby, M. T.; Asirvatham, V. S.; Kowalski, A. S.; Khan, M. A. *Organometallics* **1999**, *18*, 5004.